Negative effective-mass transition and anomalous transport in power-law hopping bands

Shimul Akhanjee*
Department of Physics, UCLA, P.O. Box 951547, Los Angeles, California 90095-1547, USA
(Received 29 January 2009; revised manuscript received 15 March 2009; published 1 May 2009)

The stability of spinless Fermions with power-law hopping $H_{ij} \propto |i-j|^{-\alpha}$ is investigated. It is shown that at precisely $\alpha_c = 2$, the dispersive inflection point coalesces with the band minimum and the charge carriers exhibit a transition into negative effective-mass regime, $m_\alpha^* < 0$ characterized by retarded transport in the presence of an electric field. Moreover, bands with $\alpha \leq 2$ must be accompanied by counter carriers with $m_\alpha^* > 0$, having a positive band curvature, thus stabilizing the system in order to maintain equilibrium conditions and a proper electrical response. We further examine the semiclassical transport and response properties, finding an infrared-divergent conductivity for $1/r$ hopping ($\alpha = 1$). The analysis is generalized to regular lattices in dimensions $d = 1$, 2, and 3.

DOI: 10.1103/PhysRevB.79.205101 PACS number(s): 71.20.−b, 71.35.−y, 73.20.At, 73.23.−b

I. INTRODUCTION

Conducting models with long-ranged power law tight-binding bands (PLTB) have been introduced in a number of different physical scenarios such as in Frenkel excitons[1] and resonating valence bond (RVB) phases.[2] Recent theoretical work on PLTB bands has focused on disorder-induced critical phenomena, where critical delocalization occurs at $\alpha = 1$ for random hopping[3,4] and a mobility edge in the regime $1 < \alpha < 3/2$ for nonrandom hopping and diagonal disorder.[1] Additionally, others have investigated variational magnetic states in strongly correlated Hubbard models at large onsite repulsion $U \gg t$ resulting in the t-J approximation with both long-ranged exchange $J_{ij} \propto |i-j|^{-2}$ and hopping[2,5,6] $t_{ij} \propto |i-j|^{-2}$. Earlier numerical investigations of nondisordered PLTB systems by Borland and Menchero[7] explored nonextensive effects of PLTB bands. They found that for finite chains of length N, in the range $0 < \alpha < 1$, there is anomalous wave packet spreading and for $\alpha > 3/2$, ballistic motion is recovered as the nearest-neighbor limit is approached. However, until now there have been no systematic studies of the dispersion relations, nor the transport properties of the nondisordered free-field model.

In this article we study various properties of PLTB chains as a function of the parameter α. Here we restrict our analysis to those particular cases of α that are tractable analytically, resulting in simple closed-form representations of the dispersion relations. The effective mass is examined as a function of α and it shown precisely that at $\alpha_c = 2$, the system enters into a negative effective-mass regime, characterized by retarded transport in the presence of an electric field. Mathematically, the critical value α_c is where the dispersive inflection point moves to the center of the Brillouin zone and the long wavelength behavior is dominated by a negative curvature. For uncoupled, isotropic tight-binding bands, the results and methods presented here can be generalized to regular lattices in dimensions 1, 2, and 3.

First let us indicate as to which energy regimes these band curvature effects play a significant role. The two primary limits to consider are near $k \to 0$ and $k = k_F$. The former case is near the band edge where the concavity and the functional form of the dispersion relation will govern the semiclassical dynamics and transport in the presence of electric and magnetic fields. However, in the latter case these curvature effects are irrelevant near the Fermi surface, where most dispersions can be expanded as follows [in one-dimensional (1D), for example]:

$$\varepsilon(\vec{k}) = \mu + \vec{v}_F(\vec{k} - \vec{k}_F) + \left.\frac{\partial^2 \varepsilon}{\partial k^2}\right|_{\vec{k}=\vec{k}_F} (\vec{k} - \vec{k}_F)^2, \qquad (1.1)$$

and the linear contribution is usually retained as $\varepsilon(k) \simeq v_F(k - k_F)$ near the Fermi points $\pm k_F$ without any loss of generality. Therefore, irrespective of the curvature away from ε_F, the low-energy Fermi surface instabilities of a PLTB model should mirror the usual nearest-neighbor model as long as the dimensionality and Fermi-surface topology remains unchanged.

II. THE NONINTERACTING BAND STRUCTURE

Consider a tight-binding model in $d = 1$ (the analysis can be generalized to higher dimensional isotropic lattices) with one orbital per site, for N sites with lattice spacing a, governed by the following Hamiltonian (neglecting spin):

$$\mathcal{H}_\alpha = -\sum_{i \neq j} t_{ij}^\alpha \psi_i^\dagger \psi_j + \text{h.c.}, \qquad (2.1)$$

where $\psi_i^\dagger$ and ψ_j are fermion fields that obey $\{\psi_i^\dagger, \psi_j\} = \delta_{ji}$. The effective width of the spectrum t_{ij} has the power-law spatial dependence,

$$t_{ij}^\alpha = \frac{t_0}{2|i-j|^\alpha}, \qquad (2.2)$$

where the constant t_0 depends on the details of the atomic-orbital overlap matrix elements. For the entirety of this article we shall focus on the specific positive integers $\alpha = 1$, 2, and 4, given that the full dispersion relations can be treated analytically, rather than only retaining asymptotic forms near the top and bottom of the band. Moreover, this particular range of exponents encompasses the earlier ranges of observed criticality in disordered systems. Note that $t_{ij}^\alpha \to 0$ as $|i-j| \to \infty$ therefore a proper convergence of the sums will

depend on k. For translationally invariant systems with periodic boundary conditions we can make use of the Bloch wave representation,

$$\psi_k = \frac{1}{\sqrt{N}} \sum_n e^{ikn} \psi_n, \tag{2.3}$$

$$\mathcal{H}_\alpha = \sum_k \varepsilon_{k,\alpha} \psi_k^\dagger \psi_k, \tag{2.4}$$

where the k's run over the first Brillouin zone. In the limit of a large system size the band dispersion takes the form

$$\varepsilon_{k,\alpha} = -t_0 \sum_{n=1}^{\infty} \sum_{z=\pm n} \frac{e^{ikz}}{|n|^\alpha} = -t_0 (\mathrm{Li}_\alpha[e^{ik}] + \mathrm{Li}_\alpha[e^{-ik}]) \tag{2.5}$$

where $\mathrm{Li}_\alpha(z)$ is the polylogarithm function.[8] For the aforementioned cases of α, one can make use of the following exactly summable series, also known as Clausen functions which are valid for $|k| < 2\pi$, which is beyond the natural cutoff of the first Brillouin zone:[8]

$$\varepsilon_{k,1} = t_0 \ln\left[2 \sin\left(\frac{|k|}{2}\right)\right], \tag{2.6}$$

$$\varepsilon_{k,2} = -t_0 \left(\frac{\pi^2}{3} - \pi|k| + \frac{k^2}{2}\right), \tag{2.7}$$

and

$$\varepsilon_{k,4} = -t_0 \left(\frac{\pi^4}{45} - \frac{\pi^2 k^2}{6} + \frac{\pi|k|^3}{6} - \frac{k^4}{24}\right). \tag{2.8}$$

Eqs. (2.6) and (2.8) have been plotted in Fig. 1. Apparently, the preceding expressions produce the full band curvature within the first Brillouin zone; however in certain cases the explicit periodicity is absent but can be repeated to construct higher Brillouin zones. Time reversal invariance is preserved such that $\varepsilon_{k,\alpha} = \varepsilon_{-k,\alpha}$. Note that the analysis can generalize to all isotropic regular lattices by simply reproducing each dispersion independently in each direction. For example, the $\alpha = 1$ case in the $d = 3$ cubic lattice can be expressed as

$$\varepsilon_{k,1}^{d=3} = t_0 \ln\left[8 \sin\frac{|k_x|}{2} \sin\frac{|k_y|}{2} \sin\frac{|k_z|}{2}\right]. \tag{2.9}$$

One will notice that the range of the hopping governs the precise functional form of the dispersion relations, especially near $k \to 0$. The first and second derivatives of $\varepsilon_{k,\alpha}$, respectively, give rise to the group-velocity $v_\alpha(k) = \frac{1}{\hbar} \frac{\partial \varepsilon_{k,\alpha}}{\partial k}$ and the effective-mass $m_\alpha^*(k) = \hbar^2 (\frac{\partial^2 \varepsilon_{k,\alpha}}{\partial k^2})^{-1}$. Taking the appropriate derivatives we have for the group velocity,

$$v_1(k) = \frac{t_0}{\hbar} \cot(|k|/2),$$

$$v_2(k) = -\frac{t_0}{\hbar}(|k| - \pi),$$

$$v_4(k) = -\frac{t_0}{\hbar}\left(-\frac{\pi^2|k|}{3} + \frac{\pi|k|^2}{2} - \frac{|k|^3}{6}\right), \tag{2.10}$$

and the effective mass in the chosen units,

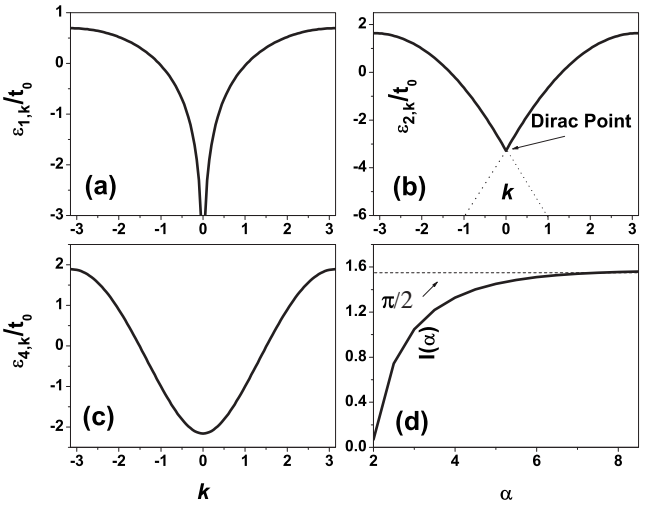

FIG. 1. A comparison of the kinetic dispersion relations at different hopping powers of α. (a) At $\alpha = 1$, there is a logarithmic divergence at $k = 0$. (b) For the case $\alpha = 2$ corresponding to inverse-squared hopping, a Dirac cone emerges at smaller values of k unlike the Tomonaga-Luttinger liquid, which is linearized around the two Fermi points $\pm k_F$, rather than at $k \to 0$. (c) At shorter-ranged hopping, the conventional parabolic band is restored, with some additional curvature. (d) Numerical determination of the inflection point $I(\alpha)$ as a function of α, where at precisely $\alpha_c = 2$, $I(\alpha_c) = 0$ (summations taken for $N = 500$).

$$m_1^*(k) = -\frac{2\hbar^2}{t_0} \sin^2(|k|/2),$$

$$m_2^*(k) = -\frac{\hbar^2}{t_0},$$

$$m_4^*(k) = -t_0 \frac{2\hbar^2}{\left(-\frac{\pi^2}{3} + \pi|k| - \frac{|k|^2}{2}\right)} \tag{2.11}$$

which have been plotted in Fig. 2. It follows that an inflection point $I(\alpha)$ can be defined as the value of k where $m_\alpha^*(k) = 0$.

III. THE NEGATIVE EFFECTIVE-MASS REGIME

A. Semiclassical dynamics

The transport of particles and holes is a well established process by which an external positive electric field will accelerate electrons of charge $e < 0$, defined to have a positive effective mass, $m_\alpha^* > 0$ from the bottom of a parabolic band.[9] On the other hand, holes with charge $e > 0$ live in a valence band with a negative curvature, and consequently an external positive electric field will accelerate these carriers in the opposite direction as the electrons, resulting in an appropriate negative effective-mass $m_\alpha^* < 0$ definition. Hence, the key point to consider is that both the concavity of a band and the charge carrier's sign will govern the direction and magnitude of a carrier's acceleration in the presence of an external field. In order to better understand the physical consequences, consider a semiclassical description in terms of the Boltzmann equation, which states that the fields $\vec{E}$ and $\vec{H}$ will change the local carrier-concentration f_k at the rate,[9]

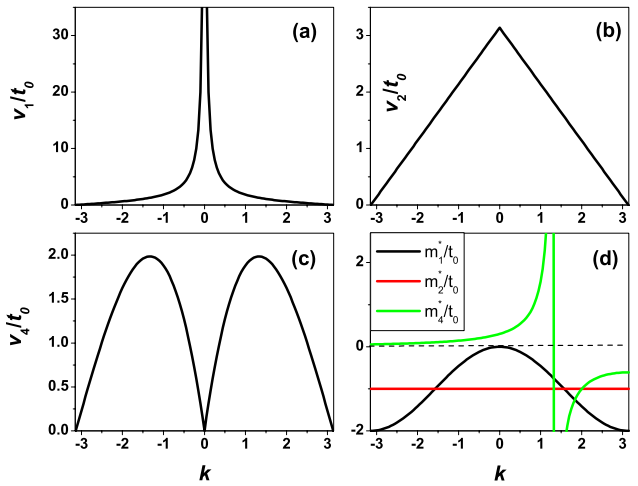

FIG. 2. (Color online) The group velocity and effective mass of the electrons ($\hbar=1$) in the chosen units (a) $\alpha=1$, the velocity diverges as the effective mass tends to zero for small k. (b) At $\alpha=2$ the velocity steadily decreases for a constant negative effective mass. (c) $\alpha=4$ is relatively short-ranged, with a velocity that increases then decreases, with a shift to negative effective-mass values originating from an inflection point in the dispersion. (d) The effective mass for each case of α. Notice the emergence of negative values at $\alpha=1,2$ for small k, where the inflection point has disappeared, and the curvature of the dispersions become purely negative.

$$\left.\frac{\partial f_{\vec{k}}}{\partial t}\right]_{\text{field}} = -\frac{d\vec{k}}{dt}\cdot\frac{\partial f_{\vec{k}}}{\partial \vec{k}} = -\frac{e}{\hbar}\left(\vec{E}+\frac{1}{c}\vec{\nabla}\varepsilon_{\vec{k},\alpha}\vec{H}\right)\frac{\partial f_{\vec{k}}}{\partial \vec{k}}. \tag{3.1}$$

Owing to the Lorenz force law, electrons and holes with reversed dispersive concavity do not have the conventional metallic response to an applied electric field; there is no acceleration of the carriers, rather the opposite occurs and the electronic transport is suppressed by a current $\mathcal{I}_<$.[10] If such carriers participate in the conduction process then a positive current recorded by the measuring instrument must be accompanied by an internal current $\mathcal{I}_o=\mathcal{I}_<+\mathcal{I}_>$, where $\mathcal{I}_>$ is part of the positive current due to particles having $m_\alpha^*>0$. Thus, in the negative effective-mass regime an experimentalist should possibly consider a multiple band structure with both types of carriers such that a net positive effective mass can maintain equilibrium.

B. Transition at $\alpha=2$

For the range of α's considered in this article, there is a definite transition in the behavior of $\varepsilon_{k,\alpha}$ from a positive to negative band curvature which can be confirmed by several different approaches. First, by only considering the exact expression given by Eq. (2.11) it is clear that $2\leq\alpha_c<4$. It follows that a complimentary numerical computation can track the behavior of the inflection point $I(\alpha)$, at a finer resolution of α's including noninteger values. The nearest-neighbor limit can be obtained at large α, having a dispersion $\varepsilon_{nn}(k)=-t_0\cos k$ with $m_\alpha^*>0$ near the band minimum and an inflection point exactly at $I_{nn}=\pm\pi/2$. Furthermore, in the nearest-neighbor limit half of the total band has a positive curvature and half has a negative curvature such that for values of $k<\pi/2$ the effective mass is $m_{nn}^*>0$ and for $k>\pi/2$, $m_{nn}^*<0$. This implies that at half filling, the entire portion of the filled band is contained within the positive effective-mass regime.

As α is decreased, I_α will drift away from $\pm\pi/2$ and a majority of the total band will have carriers with $m_\alpha^*<0$ at $k>I(\alpha)$ and a minority with $m_\alpha^*>0$ at $k<I(\alpha)$. Criticality occurs when $I(\alpha_c)=0$ and there are no sections of the filled band with a positive concavity regardless of the filling fraction.

This critical limit of interest was examined precisely by performing the summations of Eq. (2.5) numerically as shown in Fig. 1(d), where the summations converge rapidly and the finite-size effects are negligible. Notice that as α becomes smaller, the inflection point moves closer to the band center, $I(\alpha_c)=0$ until the curvature has reversed sign, at $\alpha_c\approx 2$.

Additionally, for an alternative analysis, one can make use of the derivative relation $\frac{\partial \mathrm{Li}_s(e^\mu)}{\partial\mu}=\mathrm{Li}_{s-1}(e^\mu)$. Consequently, the effective mass is controlled by the function $\mathrm{Li}_s(z)$ at negative values of s when $\alpha<2$ and in order to discern the behavior of the $\mathrm{Li}_s(z)$ function at negative indices, we can employ the expansion,[8]

$$\mathrm{Li}_{-s}(z)=\frac{1}{(1-z)^{m+1}}\sum_{k=1}^{m}a_{m,k}z^k \quad (s>0), \tag{3.2}$$

where the coefficients are Eulerian numbers that satisfy the recurrence relations,

$$a_{m,k}=(m+1-k)a_{m-1,k-1}+ka_{m-1,k}. \tag{3.3}$$

Taking the appropriate form of Eq. (2.5), it is clear that $m_\alpha^*<0$ in the range $0<\alpha<2$.

C. Transport in $1/r$ bands

For the longest ranged hopping exponent considered ($\alpha=1$), there is a unique logarithmic divergence at long-wavelength values of k, which is accompanied by a vanishing effective mass, as shown in Figs. 1(a) and 2(a), and with the reduced inertia the velocity is divergent. Such a singularity will have important consequences and requires a careful interpretation if such an equilibrium state is valid. The semiclassical conductivity tensor in the relaxation-time approximation is given by[9]

$$\sigma_\alpha^{nn'}=\frac{2}{(2\pi)^d}\frac{e^2\tau(\varepsilon_F)}{\hbar}\int_{\text{Fermi}}\frac{v_\alpha^n(k)v_\alpha^{n'}(k)d^dS_F}{v_\alpha(k)}$$

$$=\frac{2}{(2\pi)^d}\frac{e^2\tau(\varepsilon_F)}{\hbar}\int_{\text{Fermi}}\mathbf{M}^{-1}d^dS_F, \tag{3.4}$$

where the integration is taken over the Fermi surface, $\tau(\varepsilon_F)$ is the scattering lifetime at the Fermi level and $\mathbf{M}$ is the effective-mass tensor. For systems with cubic symmetry at arbitrary filling, the tensor reduces to a scalar yielding

$$\sigma_1 = \frac{2}{(2\pi)^d}\frac{e^2\tau(\varepsilon_F)}{\hbar}\int_{\text{Fermi}} v_1(k)d^dS_F = -\infty \text{ for } d = 1,2,3, \tag{3.5}$$

which is logarithmically divergent from the infrared, validating the earlier observed anomalous wave-packet spreading.[7] Moreover, a divergent conductivity will have implications in the presence of disorder, possibly explaining the critical delocalization observed in random power-law banded matrices as the quantum interference effects that usually lead to localization could be destroyed.

Another point to consider is the behavior of the Fermi-level E_F as a function of the filling fraction or density. At $\alpha=1$ the Fermi energy depends on the density ρ as

$$E_F^1(r_s) = t\ln\left(2\sin\frac{\pi\rho}{2}\right). \tag{3.6}$$

Upon inspection, Eq. (3.6) vanishes at $\rho=1/3$ or a one-third filling fraction unlike the nearest-neighbor band which has a Fermi energy that vanishes at half filling or $\rho=1/2$. In general, charge/spin-density wave formation, superconductivity, and Mott metal-insulator transitions are strongly filling fraction dependent. Therefore, it would be of interest to determine if $\rho=1/3$ is the default filling fraction in contrast to the half-filled band instabilities that are observed in the nearest-neighbor system. Furthermore, a negatively diverging Fermi energy indicates that the $\alpha=1$ system is unstable at lower densities.

D. $1/r^2$ hopping

The transition point of $\alpha=2$ is a special case of interest in different areas of Condensed matter physics. At small k, the dispersion is linear, $\varepsilon_{k,2}\propto k$, which maps onto a pseudo-relativistic kinetic energy, analogous to the six Dirac points of graphene. However, unlike the Tomonaga-Luttinger liquid, $\varepsilon_{k,2}$ is not linearized close to the two Fermi points $\pm k_F$ and does not require a cutoff in order to remedy negative-energy states.[11] It should be noted that other models that are relevant to $\alpha=2$ hopping were studied by Haldane[6] and Shastry,[5] who determined the ground state of the spin 1/2 antiferromagnetic Heisenberg chain with $1/r^2$ exchange. The Haldane-Shastry model was exactly solved by a Gutzwiller-projected wave function, identifying this particular class of inverse-squared exchange models with Anderson's RVB phase.[12] For a PLTB band the exchange constant J, in the limit of large repulsion $U \gg t$, is given by

$$J_{ij}^{\alpha} = \frac{4(t_{ij}^{\alpha})^2}{U}. \tag{3.7}$$

Thus, we emphasize that in a t-J approximation, the long-range exchange and hopping have a subtle relationship which has been overlooked, as it requires a $1/r$ kinetic band to produce a $1/r^2$ exchange constant and therefore the $1/r$ and negative effective-mass transport characteristics developed earlier in this article become important in magnetically frustrated phases. Following the work of Haldane and Shastry, Kuramoto *et al.*[2] included inverse-squared hopping in addition to inverse-squared exchange in a supersymmetric t-J model, also utilizing a Gutzwiller-projected wave function for an exact solution. Hence, the $\alpha=1,2$ cases with negative effective-mass carriers are relevant to particular classes of RVB phases and strongly correlated systems. The consequences of this apparent connection need to be explored further as the long-ranged hopping appears to control the magnetic frustration in addition to the anomalous transport characteristics shown earlier.

E. Bulk properties for $\alpha \leq 2$, $d=1$

Let us further investigate the properties of the negative effective-mass regime in 1D. Another method for probing the stability of the ground-state is to study the total energy. The emergence of a complex or imaginary component of the thermodynamic ground-state energy suggests that the system is in a nonequilibrium state. The density for a degenerate Fermi system is $\rho=k_F/\pi$ and the total kinetic energy per particle can be obtained by integrating over the internal energy distribution,

$$U_{\alpha}(\rho) = \frac{1}{N}\int_0^{E_F} \lambda g_{\alpha}(\lambda)d\lambda \tag{3.8}$$

The density of states can be easily computed by inverting the dispersion relations in terms of k and using the relation $g(\lambda)=2/\pi\hbar v(\lambda)$. After substituting the velocity expressions from Eq. (2.10), we have

$$g_1(\lambda) = \frac{2e^{\lambda/t_0}}{\pi t_0\sqrt{1-(1/4)e^{2\lambda/t_0}}}, \tag{3.9}$$

$$g_2(\lambda) = \frac{2\sqrt{3}}{\pi\sqrt{t_0(\pi^2 t_0 - 6\lambda)}}. \tag{3.10}$$

Subsequently, deep in the negative effective-mass regime, for $\alpha=1$, the total energy becomes

$$U_1(\rho) = \int_{\ln 2}^{E_F^1} \lambda g_1(\lambda)d\lambda = 2t_0\left(\frac{i\pi^2\rho^2}{4} + \pi\rho\ln[-ie^{i\pi\rho/2}] - i\text{Li}_2[-e^{-i\pi\rho}]\right) + C^1, \tag{3.11}$$

where C^1 is a complex constant. U_1 is purely real as a function of density in the range (0, 1) indicating that there are no obvious bulk instabilities. Next let us examine the ground-state energy at $\alpha=2$, which is in the critical regime. After substituting Eq. (3.10) into Eq. (3.8), we have the following density ρ-dependent ground-state energy:

$$U_2(\rho) = \int_{\pi^2/6}^{E_F^2} \lambda g_2(\lambda)d\lambda = \frac{\pi^2 t_0}{6}\{2\rho[2+\rho(\rho-3)]-1\}, \tag{3.12}$$

which is purely real, indicating a stable ground-state along with a stable Fermi energy. Lastly, the low-energy scaling in terms of the density is often used to compare with Coulomb

interactions or disorder. The well-known competition between the kinetic(band) energy and other terms can result in a change of the ground-state. Therefore, a naive low-energy scaling of the total energies results in the following:

$$U_1(\rho) \propto \ln(\rho), \tag{3.13}$$

$$U_2(\rho) \propto \rho. \tag{3.14}$$

IV. FERMI SURFACE NESTING AND SCREENING AT $\alpha=2$

Evidently, carriers with $m_\alpha^*<0$, will screen a charged impurity differently from the free Fermi gas. Therefore it would be useful to examine the susceptibility of the particle-hole channel to highlight some of these differences. The Lindhard theory is an important perturbative approach to quantify the change in the electronic charge-density δn due to a static impurity potential ϕ^{ext}. In the Appendix we present the conventional formalism used for the 1D-free Fermi gas. Here, we shall focus on the analytically tractable 1D, $T=0$ behavior of the static susceptibility $\chi_0^2(q)$ at the negative mass transition ($\alpha=2$). Substituting the form for $\varepsilon_{k,2}$ into Eq. (A2) yields the following:

$$\chi_0^2(q) = \int_{-k_F}^{k_F} \left[\frac{dk}{\varepsilon_{k+q,2} - \varepsilon_{k,2}} + \frac{dk}{\varepsilon_{k-q,2} - \varepsilon_{k,2}} \right] = \frac{1}{qt_0} \ln\left\{ \frac{[q-(2k_F+2\pi)][q-(2k_F-2\pi)]}{[q+(2k_F-2\pi)][q+(2k_F+2\pi)]} \right\}, \tag{4.1}$$

which unlike the parabolic band or nearest-neighbor case, does not exhibit a nesting singularity exactly at $q=2k_F$, rather it is shifted to $q=\pm 2(\pi-k_F)$. It follows that we can restore the lattice constant and it becomes clear that the nesting is lattice dependent, as the spacing of the reciprocal lattice determines the nesting,

$$|q| = |2k_F \pm |\vec{Q}||. \tag{4.2}$$

This dependence has further implications for the Ruderman-Kittel-Kasuya-Yosida (RKKY) function, which for a delta function impurity potential is simply the Fourier transform Eq. (4.1),

$$\delta_2 n(x) = \frac{-\sqrt{2\pi}}{t_0} \{ \text{si}[(|\vec{Q}| - 2k_F)x] - \text{si}[(|\vec{Q}| + 2k_F)x] \}. \tag{4.3}$$

Consequently at large distances we have

$$\delta_2 n(x) \propto \frac{-1}{t_0 x} \{ \cos[(|\vec{Q}| - 2k_F)x] - \cos[(|\vec{Q}| + 2k_F)x] \} \propto -\frac{\cos(|\vec{Q}|x)\sin(2k_F x)}{t_0 x}, \tag{4.4}$$

where Eq. (4.4) exhibits interference fringes (or the mathematical form of beating) instead the usual case of purely oscillatory behavior shown in Eq. (A7). Moreover, the condition for constructive interference requires that $(|\vec{Q}|-2k_F)x = 2\pi n$ for $n=0,1,2\ldots$. This suggests that in inverse-squared hopping conducting materials, the umklapp momenta can be derived from the interference fringe maxima of the Friedel oscillations. We can further examine the special case of the half-filled band where $|\vec{Q}|=4k_F$. This leads to

$$\delta_2 n(x) \propto -\frac{\cos(4k_F x)\sin(2k_F x)}{t_0 x} \tag{4.5}$$

which contains unusual $4k_F$ periodicity, reminiscent of the 1D Wigner crystal density-density oscillations.[11]

V. CONCLUSION

In summary we have explored the general dependence of the band curvature on the hopping exponent α for power-law banded electron systems, having introduced an approach that can be generalized to alternative lattices in higher dimensions. It has been shown that the curvature completely changes sign at $\alpha_c=2$ and we have determined certain static properties of system at criticality, including unusual lattice-dependent Fermi-surface nesting properties. In addition, our investigations are particularly useful for those studying Anderson localization and critical phenomena in Hamiltonians that contain long-ranged band structures as previous studies on such systems have highlighted the range $1<\alpha<1.5$ as a critical regime. Here we have demonstrated that even in the absence of disorder, the $\alpha=1$ system is not stable at lower densities and contains a logarithmic divergence of its Fermi energy and anomalous transport characteristics that may circumvent the localizing tendency of quantum interference phenomena in lower dimensional systems.

In closing we emphasize that the curvature of a band is generally associated with the magnitude and sign of the effective mass, resulting in important implications for electronic devices that require nonequilibrium conditions. For example, it has been shown that for negatively charged carriers with a negative effective mass, the current density is negative and both the Hall emf and the thermal emf are positive, which follows directly from the Lorentz force law.[10] Therefore, the capability of tuning a conducting system into a negative effective-mass regime could be exploited for technological purposes, given that the interplay of nonequilibrium conditions with disorder and quantum/thermal fluctuations can affect the critical features manifested in the transport properties. Additionally, an unexplored connection with strongly correlated models utilizing PLTB bands that lead to magnetically frustrated spin-liquid states will be explored in a future work.

ACKNOWLEDGMENTS

I would like to give thanks to Joseph Rudnick for useful discussions and assistance. Also I would like to acknowledge F. Dominguez-Adame and V. A. Malyshev for pointing out several references. This work was supported by UC General Funds (Contract. No. 4-404024-RJ-19933-02).

APPENDIX: STATIC RESPONSE OF A 1D FREE FERMI GAS

The general dielectric-response $\epsilon(q)$ can be evaluated from the following linear-response relation:

$$\epsilon(q) = \frac{\phi^{\text{ext}}(q)}{\phi(q)} = 1 - \phi^{\text{ext}}(q)\chi(q), \tag{A1}$$

where $\phi(q)$ is the full physical potential in q space and the static Lindhard response function in 1D is given by

$$\chi_0^{\alpha}(q) = 2\mathcal{P}\int \frac{dk}{2\pi}\frac{f_{k+q} - f_k}{\varepsilon_{k+q,\alpha} - \varepsilon_{k,\alpha}} \tag{A2}$$

where $\mathcal{P}$ denotes the principal part of the integral and f_k is the Fermi-Dirac distribution. For the conventional 1D noninteracting electron gas at $T=0$, this evaluates to

$$\chi_0^{nn}(q) = \frac{2m}{\pi\hbar^2 q}\ln\left|\frac{2k_F + q}{2k_F - q}\right| \tag{A3}$$

which has the well-known singularity at $q=2k_F$, associated with Fermi-surface nesting and spin/charge density-wave instabilities. In order to get a sense of the screening behavior, the simplest case assumes a delta function impurity potential of the form,

$$\phi^{\text{ext}}(x) = \frac{\hbar^2 u_0}{2m}\delta(x) \tag{A4}$$

which leads to the following real-space density modulation:

$$\delta_{\alpha} n(x) = \frac{\hbar^2}{2m}\sum_q \chi_0^{\alpha}(q)e^{iqx}. \tag{A5}$$

After substituting Eq. (A3), one has the following expression

$$\delta n_{nn}(x) = -\frac{u_0}{\pi}\int_x^{\infty}\frac{\sin t}{t}dt = -\frac{u_0}{\pi}\text{si}(2k_F x) \tag{A6}$$

which is the well-known RKKY range function. The large distance asymptotic becomes,

$$\delta n_{nn}(x) \propto -\frac{\cos(2k_F x)}{x} \tag{A7}$$

displaying the $2k_F$ periodicity and $1/x$ decay commonly referred to as Friedel oscillations.[13]

*Present address: Condensed Matter Theory Laboratory, RIKEN, Wako, Saitama, 351-0198, Japan; shimul@physics.ucla.edu

[1] A. Rodríguez, V. A. Malyshev, G. Sierra, M. A. Martín-Delgado, J. Rodríguez-Laguna, and F. Domínguez-Adame, Phys. Rev. Lett. **90**, 027404 (2003).
[2] Y. Kuramoto and H. Yokoyama, Phys. Rev. Lett. **67**, 1338 (1991).
[3] A. D. Mirlin, Y. V. Fyodorov, F.-M. Dittes, J. Quezada, and T. H. Seligman, Phys. Rev. E **54**, 3221 (1996).
[4] L. S. Levitov, Ann. Phys. **8**, 697 (1999).
[5] B. S. Shastry, Phys. Rev. Lett. **60**, 639 (1988).
[6] F. D. M. Haldane, Phys. Rev. Lett. **60**, 635 (1988).
[7] L. Borland and J. G. Menchero, Braz. J. Phys. **29**, 169 (1999).
[8] M. Abramowitz and I. A. Stegun, *Handbook of Mathematical Functions* (Dover, New York, 1970).
[9] J. M. Ziman, *Principles of the Theory of Solids*, 2nd ed. (Cambridge University Press, Cambridge, 1972).
[10] M. D. Smolin, Sov. Phys. J. **20**, 1556 (1977).
[11] T. Giamarchi, *Quantum Physics in One Dimension* (Clarendon, Oxford, 2003).
[12] P. W. Anderson, Science **235**, 1196 (1987).
[13] G. F. Giuliani, G. Vignale, and T. Datta, Phys. Rev. B **72**, 033411 (2005).